REAL-TIME IMPLEMENTATION OF A NOVEL ALGORITHM FOR ULTRASOUND FREEHAND ELASTOGRAPHY OF BREAST LESIONS

Alessandro Ramalli[1], Luca Bassi[1], Enrico Boni[1], Stefano Ricci[1], Elisabetta Giannotti[2], Dalmar Abdulcadir[2], Jacopo Nori[3], Piero Tortoli[1]

[1] Information Engineering Dept., Università degli Studi di Firenze, Italy
[2] Department of Radiology, Careggi University Hospital, Firenze, Italy
[3] Senology Diagnostic Unit, Careggi University Hospital, Firenze, Italy

ABSTRACT

The classification of breast lesions represents a main concern in current senology diagnostic practice. B-mode imaging plays a major role, but the specificity is still too low, since no information on tissue stiffness is directly provided. An original freehand elastography method, based on a Fourier domain displacement estimator, has been recently proposed and proved capable of producing off-line robust estimates of phantoms elasticity. In order to permit in-vivo examinations of breast lesions, a real-time version of the proposed method has been implemented in the research scanner ULA-OP, designed at the University of Florence. In a preliminary test on patients the proposed method detected 36 lesions (11 softer, 14 harder and 11 having the same elasticity than the surrounding tissue).The same lesions were classified as malignant (5) and benign (31) by an experienced sonographer through B-mode analysis.

Index Terms — Quasi-static elastography, Free-hand elastography, Fourier domain, Displacement estimation, real-time.

1. INTRODUCTION

Modifications of tissue's elasticity are often correlated with pathological processes: breast, prostate [1] and thyroid [2] carcinomas develop hard nodules; cirrhosis causes a diffuse reduction of liver elasticity [3], and benign lesion like cysts are typically softer than the surrounding tissue. In breast nodule detection, the simplest and most used technique is the manual palpation, but its efficacy is limited to superficial lesions of conspicuous size. Standard B-mode imaging helps especially in differentiating liquid cysts from solid breast nodules. However, B-Mode features high sensitivity but low specificity.

This work has been supported by the European Fund for Regional Development for the 2007-2013 programming period (POR FES 2007-2013 CRO MIMAUS Project) and by the Franco-Italian University (Galileo Project 2011-2012 n.26075WL).

In recent years, a new ultrasound imaging technique, elastography, has been developed [4]. It estimates the stiffness of tissues with improved sensitivity, objectivity and accuracy. In quasi-static elastography the investigated tissue is stressed by an external pressure [4]. The stress induces a strain inside the tissue which, depending on the local stiffness, produces different displacements. Such deformations can be detected comparing the echo-signals obtained in consecutive frames. In classic approaches, called coherent methods, the maximum of the cross-correlation function [4], [5], the correlation phase [6] or the weighted phase separation [7] is evaluated to estimate the displacement and differentiated to extract the strain.
The estimated strain data, color coded and displayed in a 2D map, show the relative stiffness distribution in the investigated tissue.
Recently, a new freehand quasi-static elastography method, has been introduced [8]. In this method, the axial displacement is calculated by comparing the phases of the pre- and post-compression radiofrequency (RF) signals in the frequency domain. The production of images at high frame rate (HFR) allows averaging multiple displacement estimates while maintaining the typical elastogram frame-rate of 30-40 fps. In-vitro experiments have shown that this method improves the estimate robustness with respect to a reference approach [9].
In this paper we present a real-time implementation of the novel elastography approach on the ULtrasound Advanced Open Platform (ULA-OP) [10]. The method has been validated on phantoms and then tested in-vivo in the senology unit of Careggi hospital in Florence. Examples of the real-time interface are reported.

2. METHOD

2.1. Fourier domain displacement and strain estimation

In this paragraph is concisely resumed the Fourier domain displacement estimation algorithm, which is detailed in [9].
Let us define pre- and post-compression signals, s_n and $\tilde{s}_n$, two RF signals referring to the same line on two consecutive

images during an elastography application. If such signals are sampled at a rate f_s and gated over an interval of length N_w/f_s, we obtain the sequences:

$$\begin{aligned} S_n &= \{s_n, s_{n+1}, \dots, s_{n+N_W-1}\} \\ \tilde{S}_n &= \{\tilde{s}_n, \tilde{s}_{n+1}, \dots, \tilde{s}_{n+N_W-1}\} \end{aligned} \quad (1)$$

where n is the index of the sequence and N_W is the number of points in the considered window. As reported in [5], $\tilde{S}_n$ can be usually considered as a time-shifted version of the pre-compression sequence S_n:

$$\tilde{S}_n = S_{n+\tau} \quad (2)$$

where τ is the depth-dependent time shift that has to be calculated.

Considering X_f and $\tilde{X}_f$ the discrete Fourier transform (DFT) of s_n and $\tilde{s}_n$ respectively, the proposed algorithm exploits the DFT shift theorem:

$$\tilde{X}_f = X_f e^{i\frac{2\pi}{N_W} f\tau} \quad (3)$$

to extract the time shift from the phase shift between the post- and pre-compression spectra as:

$$\tau_n = \frac{N_W \cdot \left(\arg[\tilde{X}_f] - \arg[X_f]\right)}{2\pi f} \quad \text{[samples]} \quad (4)$$

where τ_n is expressed in number of samples and can be calculated for any frequency f.

In practice, since the phase information, extracted at a single frequency, is usually noisy, it is worth averaging the time shifts calculated for N_p different frequencies around the central frequency of the signal. As the displacement and the time shift are directly correlated, the displacement gradient (strain) can be approximated by the following finite difference:

$$\Delta\tau_n = \frac{\tau_{n+1} - \tau_n}{(n+1) - n} \quad (5)$$

An elastogram is the strain calculated over the cumulative sum of successive displacement estimations.

2.2. Real-time implementation

The proposed quasi-static elastography method has been adapted to the ULA-OP architecture for its real-time implementation. In the algorithm, six logical tasks can be outlined:

1. Gating
2. Discrete Fourier transforming
3. Phases extraction
4. Displacement estimation
5. Strain estimation
6. Filtering

Of these, the most computational demanding is the discrete Fourier transform, which can be simplified as follows.

Expressing the exponential function in rectangular form, the DFT definition can be written as:

$$X_f = \sum_{n=0}^{N_W-1} s_n \left[\cos\left(\frac{2\pi}{N_W} fn\right) - i \cdot \sin\left(\frac{2\pi}{N_W} fn\right)\right] \quad (6)$$

The DFT formulation in this equation can be seen as the sum of N_W quadrature-demodulated samples of the echo signal. In order to consider all samples received from different depths, a sliding window must be applied. Equation (6) can thus be further developed as follows:

$$\begin{aligned} X_f(n) = \mathrm{FIR}_{N_W} \Big\{ s_n \Big[\cos\left(\frac{2\pi}{N_W} fn\right) - i \\ \cdot \sin\left(\frac{2\pi}{N_W} fn\right)\Big]\Big\} \cdot e^{i\phi_{f,dem}(n)} \end{aligned} \quad (7)$$

where FIR_{N_W} is a function implementing a N_W samples long finite-impulse-response filter; while

$$\phi_{f,dem}(n) = \frac{2\pi}{N_W} fn \quad (8)$$

is an additive phase term due to the quadrature demodulation.

Reducing the gating and the DFT to I/Q demodulation and FIR filtering allows any system to easily implement the elastography algorithm. In particular, on the ULA-OP the demodulation and filtering logical blocks, implemented on an FPGA (Stratix II family, Altera, San Jose, CA), is replicated 8 times (N_p=8), i.e. one for each estimation frequency. Furthermore, the spectral phases are extracted from the DFT through a lookup-table (LT), which returns the four-quadrant inverse tangent of a complex number. Then, the "arg" function used in (4) returns:

$$\arg[X_f(n)] = \mathrm{LT}[X_f(n)] - \phi_{f,dem}(n) \quad (9)$$

which computes the spectral phases and compensates them by the phase term due to the quadrature demodulation.

The displacement and strain computation are performed by the DSP (TMS320C6455, Texas Instruments, USA) as in the original form in (4) and (5), respectively. The strain is then filtered by four consecutive comb filters, which are 16-sample long each.

The elaboration results are displayed as a color scale image, called elastogram. The color palette is mapped as a function of the detected strain: blue corresponds to hard tissue, red to soft and green to normal tissue.

Depending on the compression and decompression speed, or in case of a low signal to noise ratio, the phase coherence can be lost. In order to avoid unexpected behaviors, it is important to develop a parameter (P) to assess the quality of the computed results and in turn to decide whether updating the display or not. This parameter is obtained as a function of the point τ_n variance within the 8 estimation frequencies

and a regional τ_n variance estimated over a 9×9 points area around the pixel being evaluated. The display update as a function of the parameter P is based on a persistence mechanism for each individual pixel of the elastogram. The persistence is realized by a first order IIR filter as follows:

$$y_n = P \cdot y_{n+1} + (P-1) \cdot \Delta\tau_n \quad (10)$$

where y_n is the actual value of the elastogram pixel.

2.3. Experimental setup

ULA-OP has been equipped with a 192-element linear array (LA533, Esaote SpA, Florence, Italy). The system was programmed to alternate two different modes at 6 kHz PRF. The first produces standard B-mode images, obtained by transmitting 3-cycle sine bursts at 8 MHz weighted by a Hanning window. 64 active elements were used both in transmission and in reception scanning 128 image lines (31.4 mm wide), with a 25 mm focal depth. The second mode, dedicated to elastography, used a 7-cycle burst at 7 MHz weighted with a Hanning window.
Two different elastography-dedicated phantoms were used (CIRS, model 049 and model 059, Norfolk, Virginia, USA). The first is composed of a background tissue with 29 kPa elasticity, which contains two groups of isoechoic inclusions with diameter 10 and 20 mm positioned at depths 15 and 35 mm, respectively. At each depth, two inclusions are softer and two harder than the background (6, 17, 54 and 62 kPa respectively). The second phantom mimics the US tissue behavior of the breast of a patient in supine position. This phantom contains several solid masses that appear isoechoic with respect to the surrounding tissue under normal US imaging, although the lesions are 3 times stiffer than the background. The lesions diameter range is from 3 to 10 mm.

2.4. In-vivo acquisition protocol

The proposed method has been preliminarily in-vivo tested by experienced sonographers at the Careggi University Hospital, Florence, Italy.
The patients were settled in the couch in a supine position and examined by the physician through manual palpation and a commercial US scanner in B-mode. Then, the physician used the ULA-OP scanner and located again the nodules on the real-time B-mode display. While compressing and releasing the tissue, gently moving the probe on the patients' breast, a video recording of the real-time display was saved.

3. RESULTS

Three sample frames extracted from the videos of the real-time interface are reported in Fig. 1-3. In each case, on the left the reference B-Mode image is shown while the right panel presents the elastogram overlaid on the B-Mode image.

In Fig. 1 two frames are reported, obtained while examining the elastography dedicated phantom (model 059) in the region surrounding the 62kPa hard inclusion (top) and the 6kPa soft one (bottom). A green dot is detected at the center of the soft inclusion which is due to a fabrication defect, which is even visible in the B-mode image as a white dot.
Fig. 2 shows a frame extracted during an acquisition over the breast elastography phantom, highlighting two hard inclusions placed at different depths.
In all the on-phantom examples, the inclusion are roughly visible in the B-mode while they are clearly visible in the elastograms. These images demonstrate how elastography can highlights isoechoic tissues presenting different elasticity compared to the surrounding tissue.

Real-time in-vivo acquisitions have been repeated for a total of 36 lesions (11 softer, 14 harder and 11 having the same elasticity than the surrounding tissue), classified by an experienced sonographer through B-mode analysis, as 5 malignant and 31 benign. In Fig. 3 a sample screenshot of a benign fibroadenoma in a 32 years old patient is reported. It is clearly visible both in the B-Mode image and in the elastogram, but in the latter one it is also shown as a hard nodule.

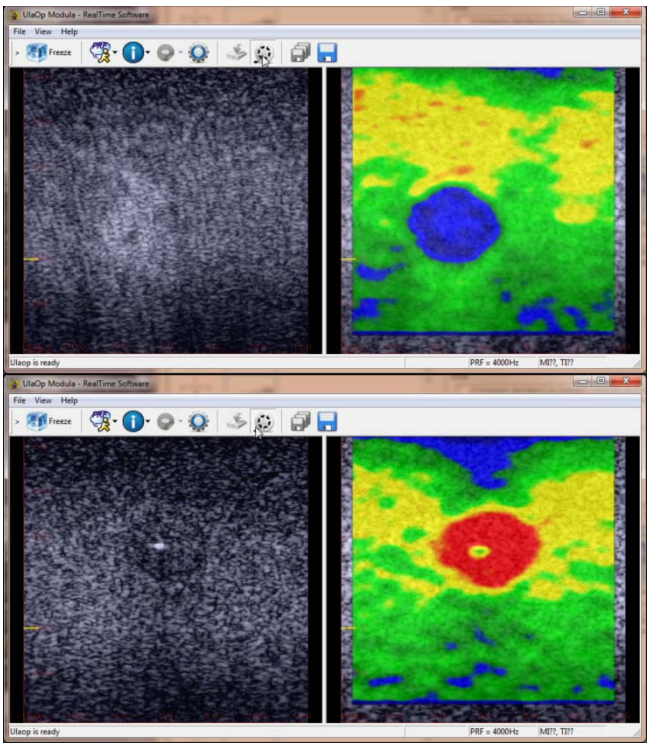

Fig. 1 Two frames extracted from the video captured from the ULA-OP real-time interface, while examining the elastography dedicated phantom (model 059) in the region surrounding the 62kPa hard inclusion (top) and the 6kPa soft one (bottom).

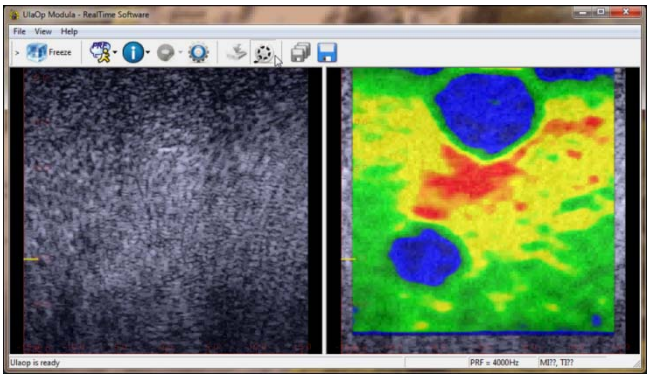

Fig. 2 A frame extracted from the video captured from the ULA-OP real-time interface during an acquisition over the breast elastography phantom, highlighting the presence of two hard inclusions.

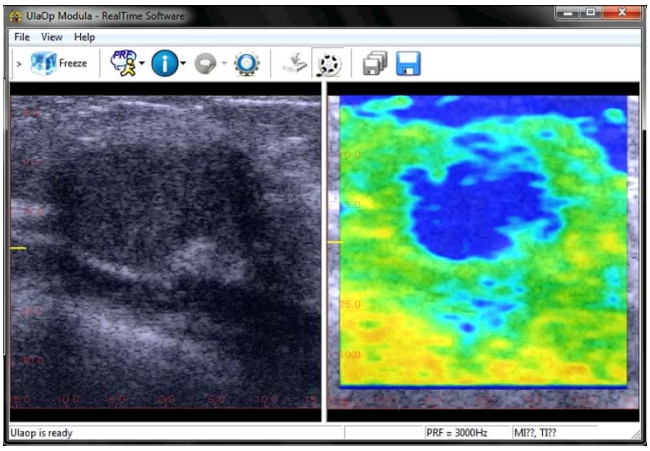

Fig. 3 A sample frame extracted from the video captured from the ULA-OP real-time interface when examining a benign fibroadenoma in a 32 years old patient.

4. DISCUSSION AND CONCLUSION

This paper has reported on the implementation of a real-time frequency domain based strain estimation algorithm for freehand elastography. The in-vivo results demonstrate the potentiality of such method as valid support for ultrasound diagnosis of breast lesions like fibroadenomas, carcinomas, cysts and nodules in general. A planned test on a larger number of patients will clarify at which extent the novel method can actually improve the diagnostic accuracy and thus reduce the biopsy assistance.

5. REFERENCES

[1] T. A. Krouskop, T. M. Wheeler, F. Kallel, B. S. Garra, and T. Hall, "Elastic moduli of breast and prostate tissues under compression," *Ultrason. Imaging*, vol. 20, no. 4, pp. 260–274, Oct. 1998.

[2] M. Dighe, U. Bae, M. L. Richardson, T. J. Dubinsky, S. Minoshima, and Y. Kim, "Differential diagnosis of thyroid nodules with US elastography using carotid artery pulsation," *Radiology*, vol. 248, no. 2, pp. 662–669, Aug. 2008.

[3] A. Kapoor, A. Kapoor, G. Mahajan, B. S. Sidhu, and V. P. Lakhanpal, "Real-time elastography in differentiating metastatic from nonmetastatic liver nodules," *Ultrasound Med. Biol.*, vol. 37, no. 2, pp. 207–213, Feb. 2011.

[4] J. Ophir, I. Céspedes, H. Ponnekanti, Y. Yazdi, and X. Li, "Elastography: a quantitative method for imaging the elasticity of biological tissues," *Ultrason. Imaging*, vol. 13, no. 2, pp. 111–134, Apr. 1991.

[5] A. Pesavento, C. Perrey, M. Krueger, and H. Ermert, "A time-efficient and accurate strain estimation concept for ultrasonic elastography using iterative phase zero estimation," *IEEE Trans. Ultrason. Ferroelectr. Freq. Control*, vol. 46, no. 5, pp. 1057–1067, Sep. 1999.

[6] M. O'Donnell, A. R. Skovoroda, B. M. Shapo, and S. Y. Emelianov, "Internal displacement and strain imaging using ultrasonic speckle tracking," *IEEE Trans. Ultrason. Ferroelectr. Freq. Control*, vol. 41, no. 3, pp. 314–325, May 1994.

[7] J. E. Lindop, G. M. Treece, A. H. Gee, and R. W. Prager, "Phase-based ultrasonic deformation estimation," *IEEE Trans. Ultrason. Ferroelectr. Freq. Control*, vol. 55, no. 1, pp. 94–111, Jan. 2008.

[8] A. Ramalli, E. Boni, O. Basset, C. Cachard, and P. Tortoli, "High frame-rate imaging applied to quasi-static elastography," in *Acoustical Imaging*, 2011, vol. 31, pp. 11–18.

[9] A. Ramalli, O. Basset, C. Cachard, E. Boni, and P. Tortoli, "Frequency-domain-based strain estimation and high-frame-rate imaging for quasi-static elastography," *Ultrason. Ferroelectr. Freq. Control IEEE Trans.*, vol. 59, no. 4, pp. 817 –824, Apr. 2012.

[10] E. Boni, L. Bassi, A. Dallai, F. Guidi, A. Ramalli, S. Ricci, R. J. Housden, and P. Tortoli, "A reconfigurable and programmable FPGA-based system for nonstandard ultrasound methods," *IEEE Trans. Ultrason. Ferroelectr. Freq. Control*, vol. 59, no. 7, pp. 1378 –1385, Jul. 2012.